Probing the Structural and Electronic Heterogeneity of $LiVPO_4F$ and $KVPO_4F$ Positive Electrode Materials by Combined X-ray Absorption and Emission Spectroscopy

Jazer Jose H. Togonon[1,2,3], Alessandro Longo[4,5], Romain Wernert[2,6,7], Lorenzo Stievano[3,6,7], Mauro Rovezzi[8], Jean-Noël Chotard[3,6,9], Antonella Iadecola[6,10*], Laurence Croguennec[2,3,6,*]

Authors' Information

[1] Synchrotron SOLEIL, L'Orme des Merisiers, Saint-Aubin, 91192 Gif-sur-Yvette, France
[2] Univ. Bordeaux, CNRS, Bordeaux INP, ICMCB, UMR 5026, F-33600 Pessac, France
[3] ALISTORE-ERI European Research Institute, FR CNRS 3104, F-80039 Amiens Cedex 1, France
[4] European Synchrotron Radiation Facility (ESRF), 71, Avenue des Martyrs, Grenoble F-38000, France
[5] Istituto per lo Studio dei Materiali Nanostrutturati (ISMN)-CNR, UOS Palermo, via Ugo La Malfa 153, Palermo 90146, Italy
[6] RS2E, Réseau Français sur le Stockage Electrochimique de l'Energie, FR CNRS #3459, Amiens F-80039 Cedex 1, France
[7] ICGM, Univ. Montpellier, CNRS, ENSCM, 34095 Montpellier, France
[8] Univ. Grenoble Alpes, CNRS, IRD, Irstea, Météo France, OSUG, FAME, F-38000 Grenoble, France
[9] Université de Picardie Jules Verne, Laboratoire de Réactivité et Chimie des Solides (LRCS), 15 rue Baudelocque, 80000, Amiens, France
[10] Sorbonne Université, PHysicochimie des Electrolytes, Nanosystèmes InterfaciauX (PHENIX), UMR CNRS 8234, 75252 Paris, France

*Corresponding authors: antonella.iadecola@synchrotron-soleil.fr, laurence.croguennec@icmcb.cnrs.fr

Keywords: Li-ion batteries, K-ion batteries, vanadium fluoride phosphate, high energy fluorescence-detected X-ray absorption near edge structure (HERFD-XANES) spectroscopy, X-ray emission spectroscopy (XES)

Supplementary Information

Table S1. Structural information including the lattice and atomic parameters of $LiVPO_4F$ (LVPF), VPO_4F-tavorite (VPF-L), $KVPO_4F$ (KVPF) [1], and VPO_4F-KTP (VPF-K) [2] obtained from Rietveld refinement of the powder XRD data.

$LiVPO_4F$ / LVPF	
Space group	*P* -1, (#2)
Z =	2
Density	3.28 g/cm^3
a =	5.1683(4) Å
b =	5.3076(4) Å
c =	7.2590(5) Å
α =	107.577(5)˚
β =	108.003(5)˚
γ =	98.357(4)˚
V =	174.17(2) Å^3
V/Z =	87.09(2) Å^3

Atom	**Wyckoff**	***x/a***	**y/b**	**z/c**	**Occ.**	**B_{iso} (Å^2)**
V1(*trans*)	*1a*	0	0	0	1	0.40(1)
V2(*trans*)	*1b*	0	0	½	1	0.31(1)
P1	*2i*	0.3288(3)	0.648(5)	0.2495(3)	1	0.56(1)
O1	*2i*	0.3703(5)	0.2350(2)	0.5865(3)	1	0.42(1)
O2	*2i*	0.1162(3)	-0.3274(6)	0.3576(3)	1	0.43(1)
O3	*2i*	0.6961(2)	0.6617(3)	-0.1358(3)	1	0.75(1)
O4	*2i*	0.2616(2)	0.7886(6)	0.0875(2)	1	0.30(1)
F1	*2i*	-0.1162(4)	0.0882(5)	0.2424(4)	1	0.84(1)
Li	*2i*	0.7160(2)	0.3700(5)	0.228(4)	1	2.64(1)

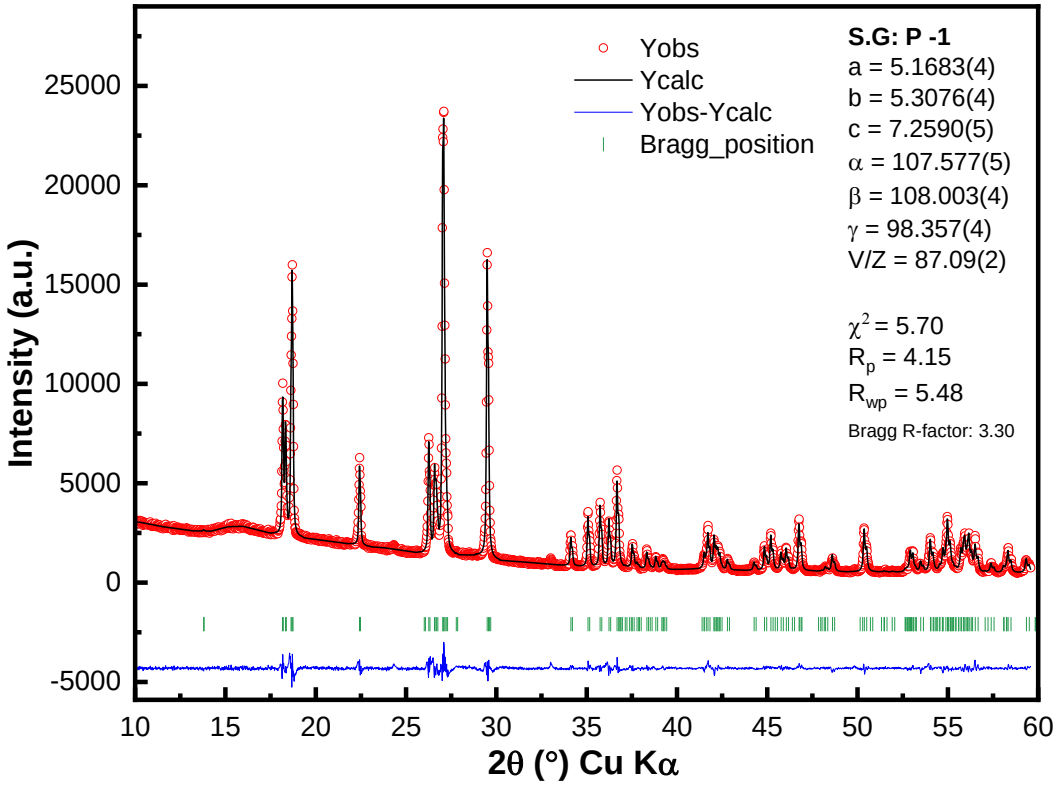

VPO_4F (tavorite) / VPF-L

Space group	*C* 2/*c*, (#15)
Z =	4
Density	3.43 g/cm^3
a =	7.1569(4) Å
b =	7.0991(2) Å
c =	7.1160(4) Å
α = γ =	90˚
β	118.069(2)˚
V =	319.02(3) Å^3
V/Z =	79.76 (2) Å^3

Atom	Wyckoff	*x/a*	y/b	z/c	Occ.	B_{iso} (Å^2)
V1	*4d*	¼	-¼	0	1	0.87(4)
P1	*4e*	½	0.1218(4)	¼	1	0.64(3)
F1	*4e*	0	-0.1664(5)	-¼	1	0.74(2)
O1	*8f*	0.3307(5)	0.0076(4)	0.0719(5)	1	0.42(3)
O2	*8f*	0.3939(8)	0.2587(5)	0.3449(7)	1	0.42(3)

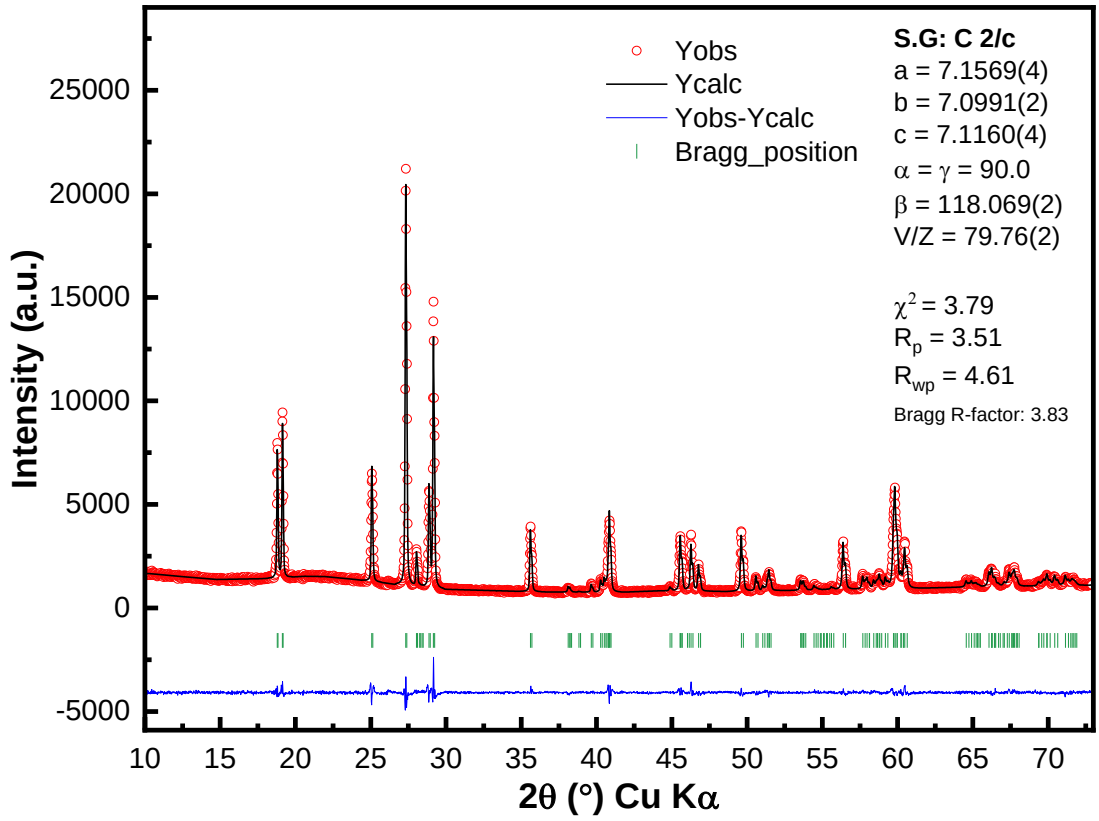

$KVPO_4F$ / KVPF

Space group	*Pna*2_1, (#33)
Z =	8
Density	3.11 g/cm^3
a =	12.8223(1) Å
b =	6.39721(3) Å
c =	10.6203(1) Å
V =	871.21(1) Å^3
V/Z =	108.90(1) Å^3

Atom	**Wyckoff**	***x/a***	**y/b**	**z/c**	**Occ.**	**B_{iso} (Å^2)**
K1	*4a*	0.3802(1)	0.7788(2)	0.3018(2)	1.02(2)	1.87(3)
K2	*4a*	0.1044(1)	0.6972(2)	0.0590(2)	0.97(2)	1.88(3)
V1(*cis*)	*4a*	0.3854(7)	0.4967(2)	0	1	0.47(1)
V2(*trans*)	*4a*	0.2469(1)	0.2514(2)	0.2469(2)	1	0.45(1)
P1	*4a*	0.4988(2)	0.3311(2)	0.2501(3)	1	0.50(1)
P2	*4a*	0.1817(1)	0.4991(4)	0.4991(3)	1	0.50(1)
O1	*4a*	0.4848(4)	0.4865(6)	0.1406(3)	1	0.44(2)
O2	*4a*	0.5122(4)	0.4682(6)	0.3691(3)	1	0.44(2)
O3	*4a*	0.4008(3)	0.1959(3)	0.2689(3)	1	0.44(2)
O4	*4a*	0.5955(3)	0.1935(6)	0.2286(5)	1	0.44(2)
O5	*4a*	0.1112(3)	0.3107(5)	0.5292(4)	1	0.44(2)
O6	*4a*	0.1127(3)	0.6910(5)	0.4722(4)	1	0.44(2)
O7	*4a*	0.2501(4)	0.5377(9)	0.6163(4)	1	0.44(2)
O8	*4a*	0.2566(4)	0.458(1)	0.3888(4)	1	0.44(2)
F1	*4a*	0.2706(4)	0.523(1)	0.8788(4)	1	0.71(4)
F2	*4a*	0.2716(4)	0.4777(9)	0.1266(4)	1	0.71(4)

VPO_4F (KTP) / VPF-K

Space group	*Pnan*, (#52)
Z =	8
Density	2.75 g/cm^3
a =	12.504(1) Å
b =	6.0875(5) Å
c =	10.462(1) Å
V =	796.32(1) Å^3
V/Z =	99.54(1) Å^3

Atom	**Wyckoff**	***x/a***	**y/b**	**z/c**	**Occ.**	**B_{iso} (Å^2)**
V1(*cis*)	*4d*	0.145(1)	¼	¾	1	1.2(2)
V2(*trans*)	*4a*	0	0	0	1	1.0(1)
P1	*4c*	¼	0.070(2)	¼	1	1.3(2)
P2	*4d*	-0.062(1)	¼	¼	1	1.3(2)
O1a	*8e*	0.246(2)	0.230(4)	-0.116(2)	1	1.2(2)
O2a	*8e*	0.149(1)	-0.067(2)	0.010(3)	1	1.2(2)
O1b	*8e*	-0.133(2)	0.051(4)	0.274(2)	1	1.2(2)
O2b	*8e*	0.010(2)	0.294(5)	0.367(2)	1	1.2(2)
F1	*8e*	0.028(2)	0.277(5)	0.626(2)	1	1.2(5)

Table S2. Summary of bond lengths of V-F and V-O for the different compounds.

LVPF	Bond length(Å)
V1-O3	1.954(6)
V1-O3	1.954(6)
V1-O4	1.957(7)
V1-O4	1.957(7)
V1-F1	1.978(8)
V1-F1	1.978(8)
V2-O1	1.924(7)
V2-O1	1.924(7)
V2-O2	2.013(7)
V2-O2	2.013(7)
V2-F1	1.998(7)
V2-F1	1.998(7)

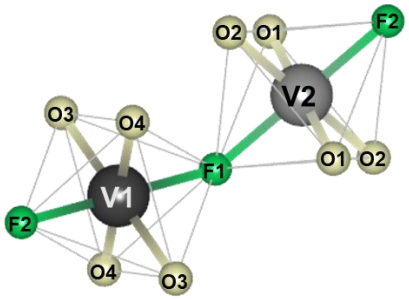

VPF-L	Bond length (Å)
V1-O1	1.913(3)
V1-O1	1.913(3)
V1-O2	1.831(6)
V1-O2	1.831(6)
V1-F1	1.930(3)
V1-F1	1.930(3)

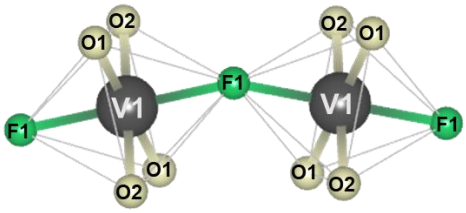

KVPF	Bond length (Å)
V1-O1	1.961(4)
V1-O2	1.928(2)
V1-O5	2.032(2)
V1-O6	1.978(4)
V1-F1	1.964(5)
V1-F2	1.984(6)
V2-O3	2.018(4)
V2-O4	1.983(2)
V2-O7	1.947(2)
V2-O8	2.010(4)
V2-F1	2.039(4)
V2-F2	1.957(4)

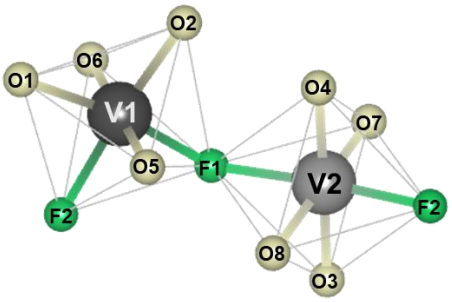

VPF-K	Bond length (Å)
V1-O1	1.895(3)
V1-O1	1.895(3)
V1-O3	1.852(5)
V1-O3	1.852(5)
V1-F1	1.951(3)
V1-F1	1.951(3)
V2-O2	1.900(2)
V2-O2	1.900(2)
V2-O4	1.879(4)
V2-O4	1.879(4)
V2-F1	1.930(4)
V2-F1	1.930(4)

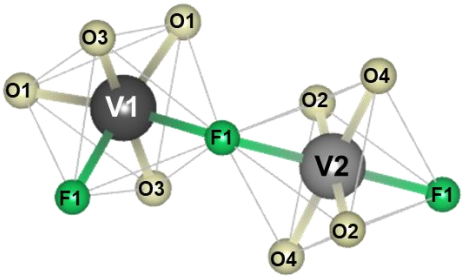

Table S3. LVPF input file for the FDMNES calculation

```
! FDMNES indata file
! Calculation for the V VtC_Kbeta LiVPO4F
! Finite difference method calculation with convolution

Filout
   pub2_output_xes/scf_cif_r10_dos/3_scf_cif_r10_lvpf

 Range     ! Energy range of calculation (eV)
 -30. 0.2 -10 0.1 -5 0.05 0. 0.05 5 0.1 10. .2 40. 1 45. ! first energy, step, intermediary
energy, step ..., last energy

 Radius    ! Radius of the cluster where final state calculation is performed
 10.0

 SCF       ! Activation of the self consistent field calculation
 Green     ! Inclusion of the green function
 Density_all   ! Densities of state results
 Edge
 K
 XES
 Z_absorber
 23
 Spgroup
 P-1

 Cif_file
 3_LiVPO4F.cif

!!!Convolution keyword : broadening with a width increasing versus energy as an arctangent

 Estart
 -20
 Efermi
 0.0
 Convolution
 42 11 10
 Gaussian
 0.7

 End
```

Table S4. VPF-L (Tavorite) input file for the FDMNES calculation

```
! FDMNES indata file
! Calculation for the V VtC_Kbeta VPO4F (tavorite)
! Finite difference method calculation with convolution

Filout
   pub2_output_xes/scf_cif_r10_dos/4_scf_cif_r10_vpf_tavor

 Range     ! Energy range of calculation (eV)
 -30. 0.2 -10 0.1 -5 0.05 0. 0.05 5 0.1 10. .2 40. 1 45. ! first energy, step, intermediary
energy, step ..., last energy

 Radius    ! Radius of the cluster where final state calculation is performed
 10.0

 SCF       ! Activation of the self consistent field calculation
 Green     ! Inclusion of the green function
 Density_all   ! Densities of state results
 Edge
 K
 XES
 Z_absorber
 23
 Spgroup
 15:b1

 Cif_file
 4_VPO4F-Tavorite.cif

!!!Convolution keyword : broadening with a width increasing versus energy as an arctangent

 Estart
 -20
 Efermi
 0.0
 Convolution
 42 11 10
 Gaussian
 1.2

 End
```

Table S5. KVPF input file for the FDMNES calculation

```
! FDMNES indata file
! Calculation for the V VtC_Kbeta KVPO4F
! Finite difference method calculation with convolution

Filout
   pub2_output_xes/scf_cif_r10_dos/1_scf_cif_r10_kvpf

 Range     ! Energy range of calculation (eV)
 -30. 0.2 -10 0.1 -5 0.05 0. 0.05 5 0.1 10. .2 40. 1 45. ! first energy, step, intermediary
energy, step ..., last energy

 Radius    ! Radius of the cluster where final state calculation is performed
 10.0

 SCF       ! Activation of the self consistent field calculation
 Green     ! Inclusion of the green function
 Density_all   ! Densities of state results
 Edge
 K
 XES
 Z_absorber
 23
 Spgroup
 33

 Cif_file
 1_KVPO4F.cif

!!!Convolution keyword : broadening with a width increasing versus energy as an arctangent

 Estart
 -20
 Efermi
 0.0
 Convolution
 42 11 10
 Gaussian
 1.2

 End
```

Table S6. VPF-K input file for the FDMNES calculation

```
! FDMNES indata file
! Calculation for the V VtC_Kbeta VPO4F (KTP)
! Finite difference method calculation with convolution

Filout
   pub2_output_xes/scf_cif_r10_dos/2_scf_cif_r10_vpf_ktp

 Range     ! Energy range of calculation (eV)
 -30. 0.2 -10 0.1 -5 0.05 0. 0.05 5 0.1 10. .2 40. 1 45. ! first energy, step, intermediary
energy, step ..., last energy

 Radius    ! Radius of the cluster where final state calculation is performed
 10.0

 SCF       ! Activation of the self consistent field calculation
 Green     ! Inclusion of the green function
 Density_all   ! Densities of state results
 Edge
 K
 XES
 Z_absorber
 23
 Spgroup
 52:a-cb

 Cif_file
 2_VPO4F-KTP.cif

!!!Convolution keyword : broadening with a width increasing versus energy as an arctangent

 Estart
 -20
 Efermi
 0.0
 Convolution
 42 11 10
 Gaussian
 1.2

 End
```

Table S7. Calculated bond valence sum (BVS) for the pristine materials and their respective deintercalated phases.

	V(1)	V(2)	$V_{average}$
LVPF	3.10	3.17	**3.14**
VPF-L	4.12	-	**4.12**
KVPF	3.10	2.96	**3.03**
VPF-K	4.03	3.95	**3.99**

Bonding	*Ro*	*b*
V^{III}-$O^{(-2)}$	1.743	0.37
V^{III}-$F^{(-1)}$	1.702	
V^{IV}-$O^{(-2)}$	1.784	
V^{IV}-$F^{(-1)}$	1.700	

$$BVS = \sum_{R_{exp}=1}^{6} e^{\frac{R_o - R_{exp}}{b}}$$

Table S8. Calculated distortion index for the pristine materials and their respective deintercalated phases.

The distortion index is an estimate of the deviation from a regular octahedron and was calculated using the formula below:

	$\bar{d}_{V(1)}$	Distortion index V(1)	$\bar{d}_{V(2)}$	Distortion index V(2)
LVPF	1.963(7)	2.96 x 10^{-5}	1.978(7)	3.87 x 10^{-4}
VPF-L	1.891(4)	5.19 x 10^{-4}		
KVPF	1.975(4)	2.52 x 10^{-4}	1.993(4)	2.74 x 10^{-4}
VPF-K	1.903(3)	4.56 x 10^{-4}	1.899(4)	1.24 x 10^{-4}

$$Distortion\ index = \frac{1}{6}\sum_{i=1}^{6}\frac{(d_i - \bar{d})^2}{\bar{d}^2}$$

Where d_i corresponds to each V-X bond of the octahedron and $\bar{d}$ is the average bond length

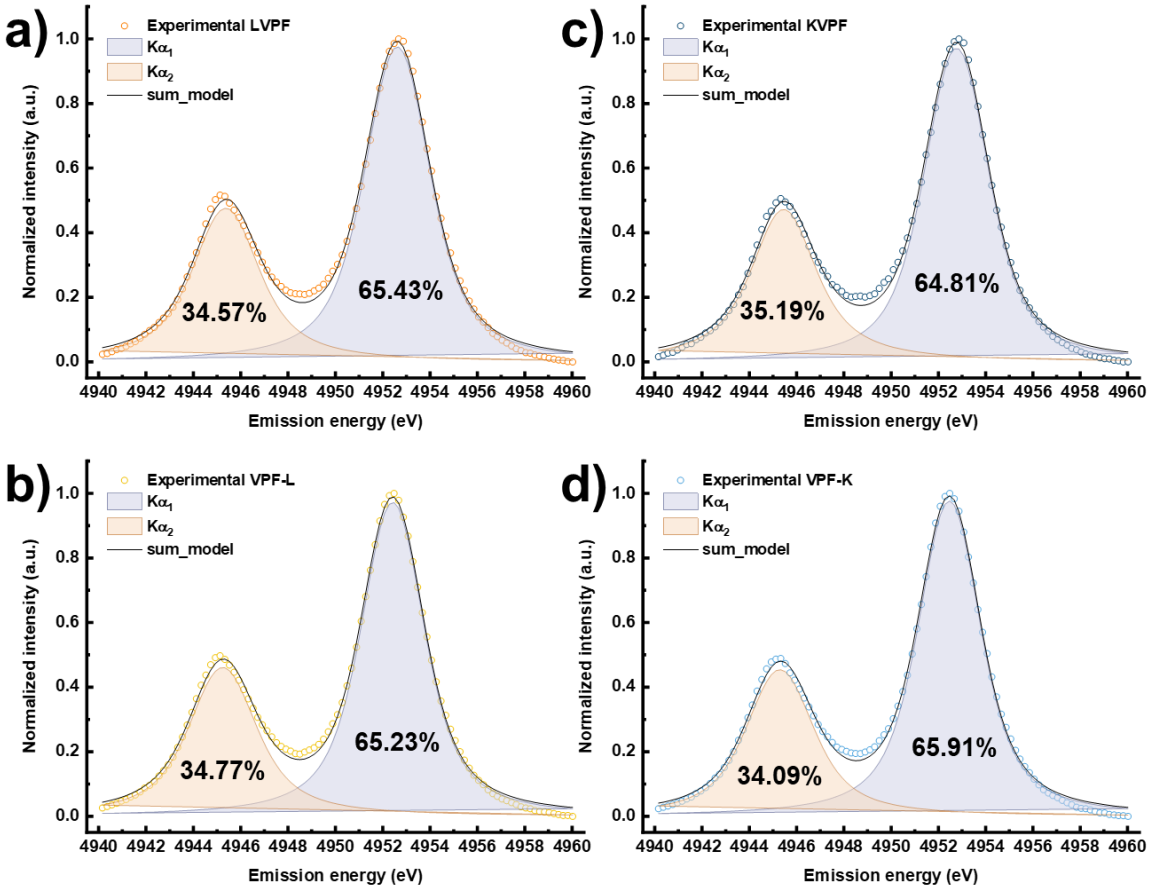

Figure S1. The deconvolution of CtC Kα emission line using two symmetrical Voigt functions for a) LVPF, b) VPF-L, c) KVPF, and d) VPF-K

Table S9. Summary of the Curve-fitting parameters and calculated contributions of CtC Kα

LVPF	Position, eV	FWHM, eV	Area, %	Gaussian FWHM, eV	Lorentzian FWHM, eV	Weighted Sum of Squared Residuals
$K\alpha_1$	4952.62	3.32	65.43	2.03	2.03	1.03×10^{-2}
$K\alpha_2$	4945.37	3.41	34.57	1.64	2.57	

VPF-L	Position, eV	FWHM, eV	Area, %	Gaussian FWHM, eV	Lorentzian FWHM, eV	Weighted Sum of Squared Residuals
$K\alpha_1$	4952.42	3.19	65.23	1.93	1.97	1.29×10^{-2}
$K\alpha_2$	4945.24	3.45	34.77	1.78	2.48	

KVPF	Position, eV	FWHM, eV	Area, %	Gaussian FWHM, eV	Lorentzian FWHM, eV	Weighted Sum of Squared Residuals
$K\alpha_1$	4952.77	3.28	64.81	2.07	1.92	3.10×10^{-2}
$K\alpha_2$	4945.48	3.37	35.19	1.38	2.75	

VPF-K	Position, eV	FWHM, eV	Area, %	Gaussian FWHM, eV	Lorentzian FWHM, eV	Weighted Sum of Squared Residuals
$K\alpha_1$	4952.46	3.17	65.91	1.90	1.98	2.91×10^{-2}
$K\alpha_2$	4945.29	3.44	34.09	1.87	2.37	

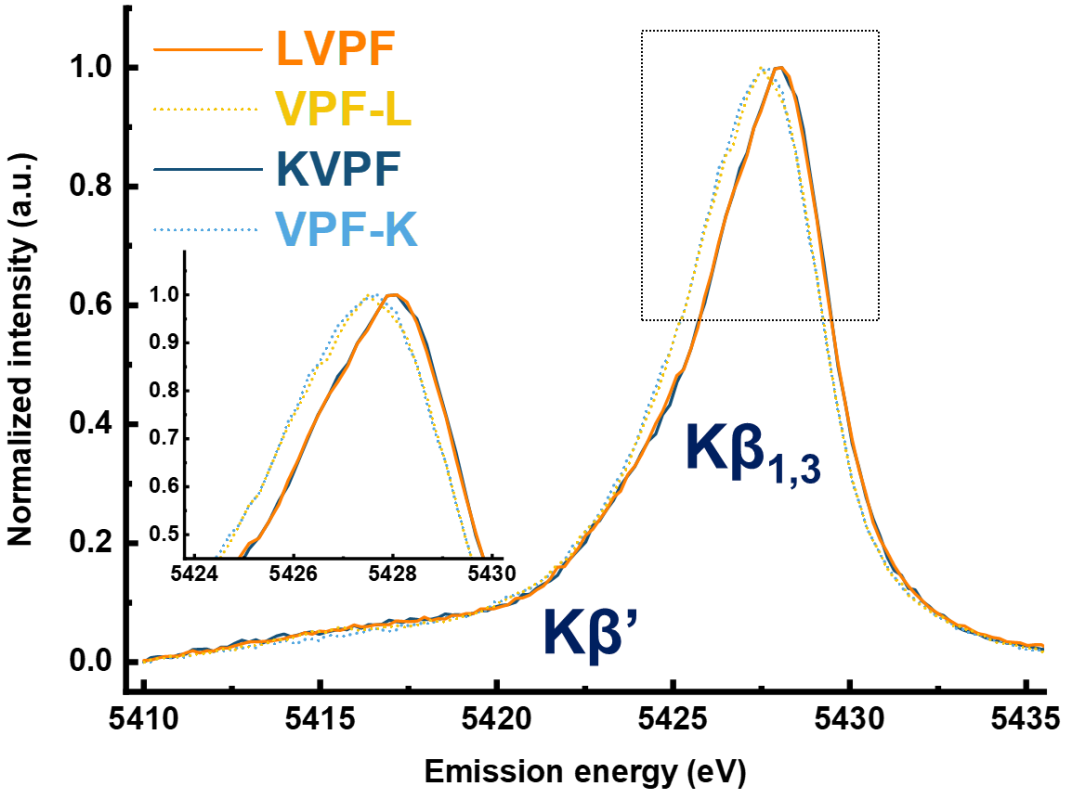

Figure S2. The CtC Kβ X-ray emission lines of the pristine LVPF and KVPF, and their corresponding deintercalated phases, VPF-L and VPF-K. Inset shows the maximum peak position at the $K\beta_{1,3}$.

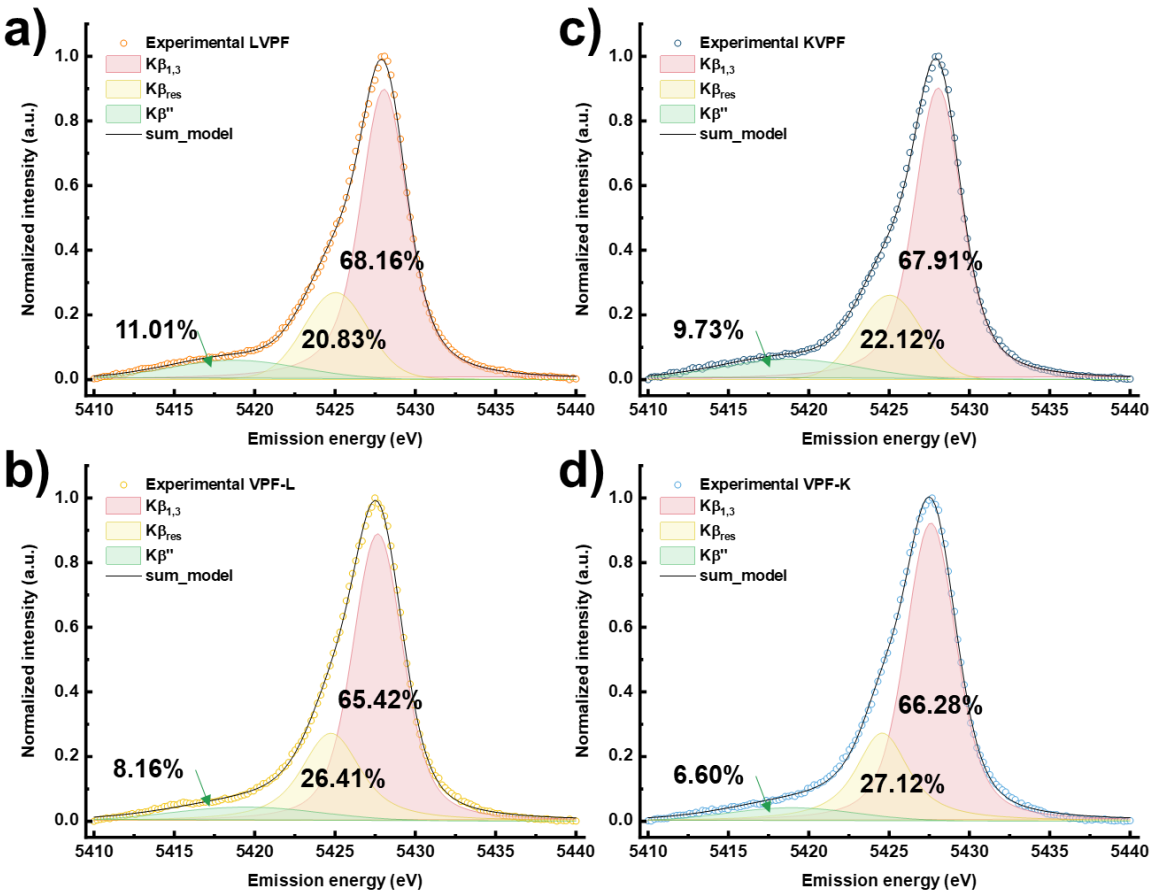

Figure S3. The deconvolution of CtC Kβ emission line using three symmetrical Voigt functions for a) LVPF, b) VPF-L, c) KVPF, and d) VPF-K

Table S10. Summary of the Curve-fitting parameters and calculated contributions of CtC Kβ

LVPF	Position, eV	FWHM, eV	Area, %	Gaussian FWHM, eV	Lorentzian FWHM, eV	Weighted Sum of Squared Residuals
$K\beta_{1,3}$	5428.05	3.53	68.16	2.34	1.91	0.75×10^{-6}
$K\beta_{res}$	5425.03	4.64	20.83	4.64	0.45	
Kβ"	5418.83	10.13	11.01	10.06	0.12	

VPF-L	Position, eV	FWHM, eV	Area, %	Gaussian FWHM, eV	Lorentzian FWHM, eV	Weighted Sum of Squared Residuals
$K\beta_{1,3}$	5427.66	3.71	65.42	2.83	1.50	1.81×10^{-6}
$K\beta_{res}$	5424.75	4.34	26.41	2.27	3.09	
Kβ"	5419.44	11.02	8.16	10.95	0.13	

KVPF	Position, eV	FWHM, eV	Area, %	Gaussian FWHM, eV	Lorentzian FWHM, eV	Weighted Sum of Squared Residuals
$K\beta_{1,3}$	5428.05	3.51	67.91	2.28	1.98	2.03×10^{-6}
$K\beta_{res}$	5425.03	4.63	22.12	4.42	0.38	
Kβ"	5418.74	9.73	9.97	9.72	0.01	

VPF-K	Position, eV	FWHM, eV	Area, %	Gaussian FWHM, eV	Lorentzian FWHM, eV	Weighted Sum of Squared Residuals
$K\beta_{1,3}$	5427.60	3.75	66.28	2.83	1.55	1.04×10^{-6}
$K\beta_{res}$	5424.57	3.91	27.12	2.52	3.28	
Kβ"	5418.93	9.45	6.60	9.41	0.07	

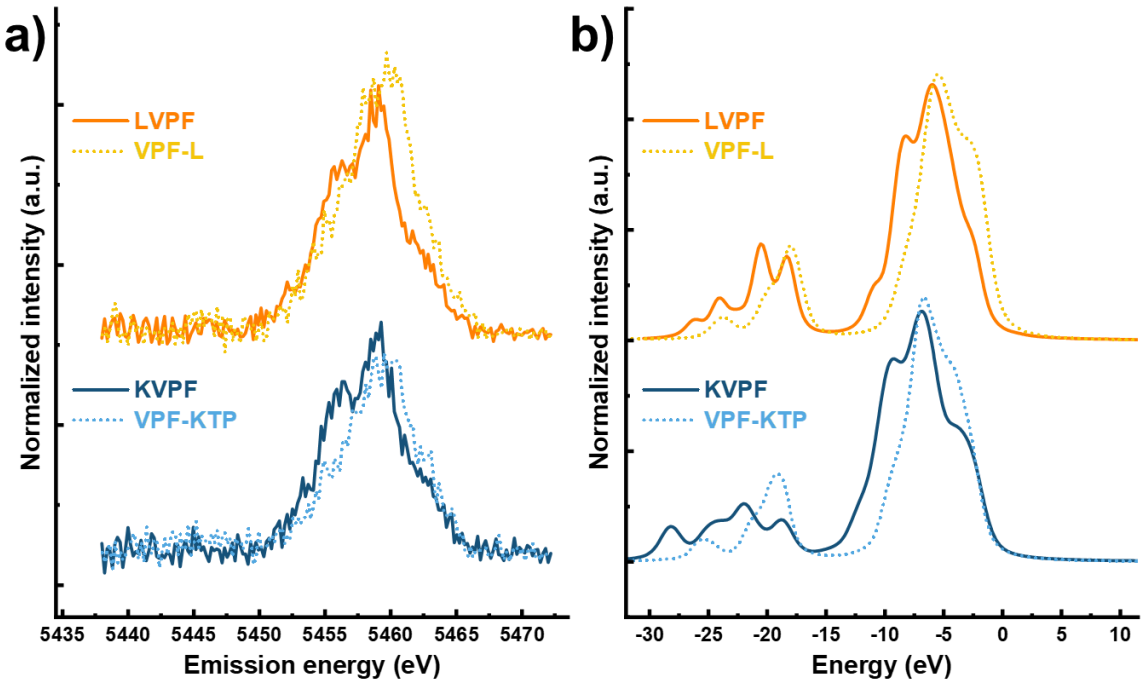

Figure S4. The a) experimental and b) simulated XES VtC Kβ emission line of LVPF, VPF-L, KVPF, and VPF-K. Overall features obtained especially at the VtC $K\beta_{2,5}$ are in good agreement with our previous work. [3]

References

[1] R. Wernert, L.H.B. Nguyen, E. Petit, P.S. Camacho, A. Iadecola, A. Longo, F. Fauth, L. Stievano, L. Monconduit, D. Carlier, L. Croguennec, Controlling the Cathodic Potential of KVPO 4 F through Oxygen Substitution, Chem. Mater. 34 (2022) 4523–4535. https://doi.org/10.1021/acs.chemmater.2c00295.

[2] R. Wernert, L.H.B. Nguyen, A. Iadecola, F. Weill, F. Fauth, L. Monconduit, D. Carlier, L. Croguennec, Self-Discharge Mechanism of High-Voltage KVPO 4 F for K-Ion Batteries, ACS Appl. Energy Mater. 5 (2022) 14913–14921. https://doi.org/10.1021/acsaem.2c02379.

[3] J.J.H. Togonon, A. Iadecola, R. Wernert, K. Choudhary, M. Rovezzi, J.-N. Chotard, L. Stievano, A. Longo, L. Croguennec, Disentangling the ligand and electronic structure in KVPO4F1-xOx positive electrode materials by Valence-to-Core X-ray emission spectroscopy, Energy Storage Mater. 69 (2024) 103406. https://doi.org/10.1016/j.ensm.2024.103406.